PROPOSED TRANSPORT BEAM LINE FOR DESIR

by

Dragan TOPREK

Laboratory for Nuclear and Plasma Physics, Vinča Institute of Nuclear Sciences,
University of Belgrade, Belgrade, Serbia

Scientific paper
DOI: 10.2298/NTRP1403171T

In this paper the detailed structure of the transport beam line design is proposed, quadrupoles and deflectors specifications in order to transport the beam from the optic adaptation point in the SPIRAL2 production building up to the adaptation point in the DESIR hall. All optical elements, in beam line, are electrostatic and so, settings are independent of the ratio q/m of the particle. The calculations are done by COSY INFINITY computer code in first order of approximation and without fringe field effects. The beam emittances at the starting point (adaptation point in the SPIRAL2 production building) in horizontal and vertical planes are 80 mm mrad. The beam line is designed in such a way that the beam sizes, in both planes, at the end (adaptation point in the DESIR hall) are kept the same as they are at the starting point; the horizontal and vertical displacements from the optic axis at starting and ending points are the same, 6 mm. In such case the efficiency of transport of the beam is high.

Key words: beam line, emittance, ion optics, COSY INFINITY

INTRODUCTION

The advent of radioactive beam facilities has given a new impetus to nuclear structure physics during the last two decades [1, 2]. It has led to several major unexpected discoveries such as the existence of dilute neutron matter in halo nuclei, the modification of shell structure and magic numbers far from stability, proton and two-proton radioactivity, and new regions of shape coexistence. There are two main methods for producing radioactive ion beams: projectile fragmentation and isotope separation on-line (ISOL). The fragmentation facility will be facility for antiproton and ion research (FAIR) [3] in Darmstadt, Germany, while the ISOL facility is named European isotope separation on-line (EURISOL) [4]. The technical challenges for EURISOL were found to be too great to envisage rapid construction and a European roadmap towards the ultimate facility EURISOL was proposed. This plan encompasses the construction of three intermediate generation ISOL facilities: HIE ISOLDE (isotope separation on-line detector) at CERN [5], SPES (selective production of exotic species) at Legnaro [6] and the most ambitious of the three, SPIRAL2 (Système de Production d'Ions Radioactifs en Ligne de 2^{e} Generation) at GANIL (Grand Accélérateur National d'Ions Lourds).

* Corresponding author; e-mail: toprek@vinca.rs

The SPIRAL2 facility at GANIL will produce radioactive isotopes ranging from the lightest, to very heavy elements beyond uranium [7]. Different production mechanisms will be utilized [8]: fission of ^{238}U to produce medium-mass, neutron-rich isotopes, fusion evaporation for medium-mass, neutron-deficient nuclei, and transfer and deep-inelastic reactions for light to heavy nuclei closer to the line of β stability.

In this paper the detailed structure is proposed, quadrupoles and deflectors specifications in order to transport the beam from the optic adaptation point in the SPIRAL2 production building up to the adaptation point in the DESIR (Desintegration, Excitation et Stockage d'Ions Radioactifs) hall.

ION OPTICS OF TRANSPORT BEAM LINE

Transport beam line starts with LRD-Q501 electrostatic quadrupole and ends with ARD-Q14 electrostatic quadrupole (included drifts before LRD-Q501 and after ARD-Q14 quadrupoles). The schematic view of this line is shown in fig. 1. All optical elements are electrostatic and so, settings are independent of the ratio q/m of the particle. The calculations are done by COSY INFINITY [9] ion-optical code in first order of approximation and without fringe field effects. The phase space dimensionality used was 2, being the x-a (horizontal plane) as well as y-b (vertical plane) mo-

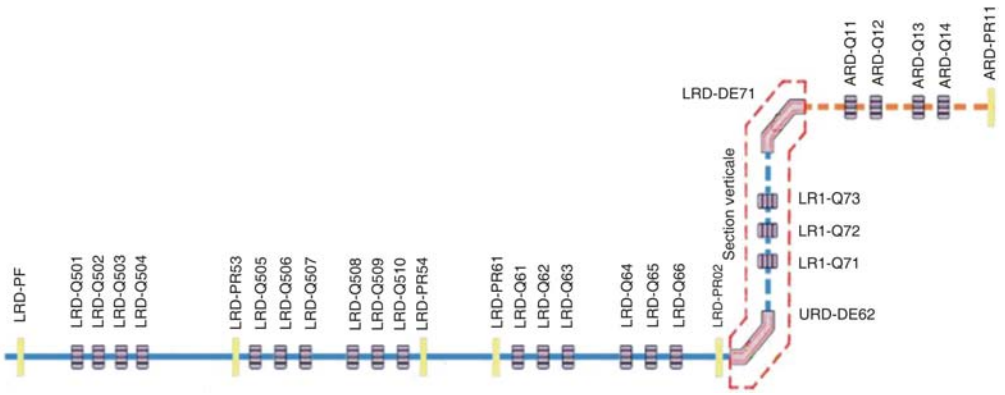

Figure 1. The layout of the transport beam line. In this paper, the transport beam line from adaptation point in the SPIRAL2 production building (optical element marked by LRD-Q501, included drift before LRD-Q501 quadrupole) is studied, up to the adaptation point in the DESIR hall ([7, 10] optical element marked by ARD-Q14, included drift after ARD-Q14 quadrupole). The rest of the elements shown in this picture marked as LRD-PF, LRD-PR53, LRD-PR54, LRD-PR61, LRD-PR62, and ARD-PR11 are beam profile monitors)

tion computed. Here a and b are the angles between paraxial rays and optic axis in horizontal and vertical planes, respectively.

For the reference particle, the particle with mass (m_0) 122 amu is chosen, with charge (Z_0) 1 ($^{122}Sn^+$), electrostatic rigidity of 0.121 MV and kinetic energy (K_0) of 60 keV. It is considered the particle with relative mass deviation $dm/m_0 = 2\ 10^{-4}$, relative kinetic energy deviation $dK/K_0 = 2\ 10^{-4}$, and relative charge deviation $dZ/Z_0 = 0$. The starting points of this particle in the initial horizontal and vertical phase spaces are

$$x_0 \quad y_0 \quad 6 \text{ mm}$$

$$a_0 \quad b_0 \quad 13.333 \text{ mrad}$$

which corresponds to the beam emittance [9, 11] in horizontal and vertical plane $\varepsilon_x = \varepsilon_y = 80$ mm mrad. x_0 and y_0 are the horizontal and vertical displacements from the optic axis, a_0 and b_0 are the angles between paraxial ray and optic axis in horizontal and vertical planes, respectively.

Kinetic energy (K_0), mass (m_0), and charge (Z_0) of the reference ion are used as parameters in the code COSY INFINITY and thus all calculations are performed in the following scaled co-ordinates [9, 11]

$$x$$
$$a \quad \frac{p_x}{p_0}$$
$$y$$
$$b \quad \frac{p_y}{p_0}$$
$$\delta_K \quad \frac{K - K_0}{K_0}$$
$$\delta_m \quad \frac{m - m_0}{m_0}$$
$$\delta_Z \quad \frac{Z - Z_0}{Z_0}$$

where p_0 is the total momentum of the reference ion and p_x and p_y are its horizontal and vertical components, respectively.

It should be emphasized here that horizontal plane is the bending plane; *i. e.*, the plane of the drawing in fig. 1 and it does not correspond to the horizontal plane in the laboratory system. The Twiss parameters [11] at the starting point are

$$a_{x0} \quad a_{y0} \quad 0$$
$$\beta_{x0} \quad \frac{x_0}{a_0} \quad \frac{x_0^2}{\varepsilon_x}$$
$$\beta_{y0} \quad \frac{y_0}{b_0} \quad \frac{y_0^2}{\varepsilon_y}$$

Three basic principles were considered in the design of the beam line:

– achieving point-to-point imaging in the beam transport from one section to the following, so that phase space properties of the beam become simpler; such an arrangement is also beneficial for the reduction of the beam halo and thus the experimental background by placing baffle slits at the focusing points,
– placing the ion-optical elements as symmetrically as possible, so that the adjustment of the beam line parameters becomes simpler; symmetrical arrangement is associated with the benefit of smaller aberrations, and
– keeping in mind the availability of the space since the beam line must be fitted by the existing facilities and buildings.

The whole beam line is divided in 5 sub-sections. First sub-section (fig. 1) consists of the four electrostatic quadrupoles; LRD-Q501, LRD-Q502, LRD-Q503, and LRD-Q504, arranged in the following way

$$L_1 / \ k_1^{Q501} / L_2 / \ k_2^{Q502}$$
$$/ L_3 / \ k_2^{Q503} / L_2 / \ k_1^{Q504} / L_1$$

where L_1 is the length of the drifts before LRD-Q501 and after LRD-Q504 quadrupoles, L_2 – the distance

between LRD-Q501 and LRD-Q502 quadrupoles (distance between LRD-Q503 and LRD-Q504 is also L_2), L_3 – the distance between LRD-Q502 and LRD-Q503 quadrupoles, and k – the strength of the quadrupole given by (ref. 11, page 48)

$$k \quad \sqrt{\frac{2V}{R_0^2 \chi}} \tag{1}$$

where χ, R_0, and V describe the rigidity of the particle, the half of the aperture of the quadrupole and the electrostatic potential at the pole tip, respectively. In our case $k_1^{(Q501)}$ and $k_1^{(Q504)}$ mean that the strengths of LRD-Q501 and LRD-Q504 quadrupoles are the same but opposite in sign. Similarly, the strengths of LRD-Q502 and LRD-Q503 are also the same but opposite in sign. The similar notation will be used for the other sub-sections.

The beam optics of the first sub-section are shown in figs. 2(a and b). The total length of the first sub-section $L_{T,1}$ is 4.642 m. The potentials at pole tips of all quadrupoles are fitted to get the beam size in the both transversal planes to be equal and to be $x = x_0 = 6$ mm and $y = y_0 = 6$ mm and, also, the matrix elements σ_{21} and σ_{43} of the beam matrix have to be zeroed; to ensure the beam waist at the end of this section. The transfer matrix T_1 at the end of the first sub-section is

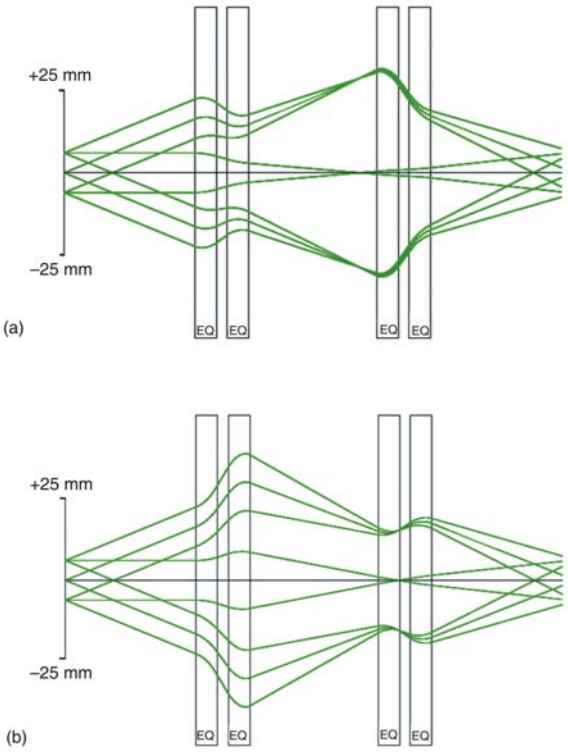

Figure 2. The beam optics of the first sub-section in the bending plane (a) and the beam optics of the first sub-section in the vertical plane (b)

$$T = \begin{pmatrix} 0.9648 & 0.5842 & 0 & 0 \\ 0.1182 & 0.9648 & 0 & 0 \\ 0 & 0 & 0.9648 & 0.5842 \\ 0 & 0 & 0.1182 & 0.9648 \end{pmatrix} \tag{2}$$

The magnifications in x-plane (bending plane) M_x $T_1(1, 1)$ and in y-plane (transversal plane) M_y $T_1(3, 3)$ are equal

$$M_x = M_y$$

The distances L_1, L_2, L_3, and the potentials at the pole tip of LRD-Q501, LRD-Q502, LRD-Q503, and LRD-Q504 quadrupoles are: L_1 = 1.221 m, L_2 = = 0.100 m, L_3 = 1.200 m, $V_{Q501} = -V_{Q504} = -1.2437$ kV, $V_{Q502} = -V_{Q503}$ = 1.4635 kV. The length ℓ of each quadrupole is 20 cm, and the half of the aperture R_0 of each quadrupole is 5 cm. The total length of the first sub-section $L_{T,1}$ is 4.642 m.

The second sub-section consists of two electrostatic quadrupole triplets arranged in a symmetrical way; *i. e.*

$$L_4 / \ k_3^{Q505} / L_2 / \ k_4^{Q506} / L_2 / \ k_3^{Q507} / L_5 / \ k_3^{Q508} / L_2 / \ k_4^{Q509} / L_2 / \ k_3^{Q510} / L_4$$

where L_4 is the length of the drifts before the LRD-Q505 and after LRD-Q510 quadrupoles, L_2 – the mutual distances of the quadrupoles of the each triplets, L_5 – the distance between LRD-Q507 and LRD-Q508 quadrupoles, k – the strength of the quadrupoles given by eq. (1). From the arrangement of the second sub-section it can be seen that the strength of LRD-Q505, LRD-Q507, LRD-Q508, and LRD-Q510 quadrupoles are the same. Also, the strength of the LRD-Q506 and LRD-Q509 are the same. The total length of the second sub-section $L_{T,2}$ is 5.800 m. The potentials at pole tips of quadrupoles are fitted to vanish the diagonal elements of the $T_2^{0,C}$ matrix (the matrix at the center of only the 2nd sub-section; the first sub-section is excluded); $T_2^{0,C}(1, 1) = 0$, $T_2^{0,C}(2, 2) = 0$, $T_2^{0,C}(3, 3) = 0$, and $T_2^{0,C}(4, 4) = 0$. The transfer matrix $T_2^{0,C}$ at the end of this sub-section, when the first sub-section is excluded, is

$$T_2^0 = \begin{pmatrix} 1.0000 & 2.132\ 10^{13} & 0 & 0 \\ 0.5795\ 10^{13} & 1.0000 & 0 & 0 \\ 0 & 0 & 1.0000 & 0.8216\ 10^{14} \\ 0 & 0 & 0.1354\ 10^{13} & 1.0000 \end{pmatrix} \tag{3}$$

The transfer matrix T_2 at the end of the 2nd sub-section, when the first sub-section is included, is

$$T_2 = \begin{pmatrix} 0.9648 & 0.5842 & 0 & 0 \\ 0.1182 & 0.9648 & 0 & 0 \\ 0 & 0 & 0.9648 & 0.5842 \\ 0 & 0 & 0.1182 & 0.9648 \end{pmatrix} \tag{4}$$

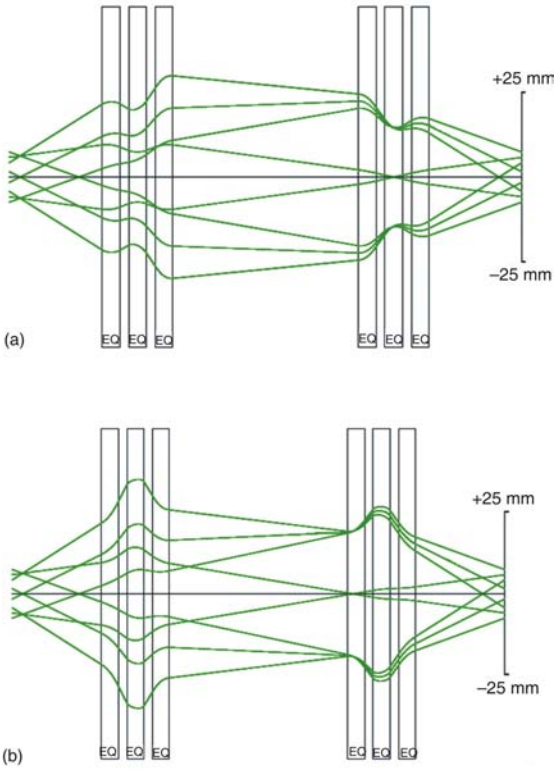

Figure 3. The beam optics of the second sub-section in the bending plane (a) and the beam optics of the second sub-section in the vertical plane (b)

By comparing the matrices at the end of the first and the second sub-sections this relation can be noticed

$$T_2 = -T_1 \tag{5}$$

The distances L_4 and L_5 and the potentials at the pole tips of quadrupoles are: L_4 = 1.050 m, L_5 = = 2.100 m, $V_{Q505} = V_{507} = V_{Q508} = V_{Q510} = -1.0724$ kV, $V_{Q506} = V_{Q509} = 1.9787$ kV. The length ℓ and the half of the aperture R_0 of each quadrupole are same as in the first sub-section; 20 cm and 5 cm, respectively. The beam optics of the second sub-section are shown in figs. 3(a and b).

The structure of the third sub-section is the same as the structure of the second one, *i. e.*, the third sub-section consists of two electrostatic quadrupole triplets arranged in a symmetrical way, *i. e.*

$$L_6 / \ k_5^{Q61} / L_2 / \ k_6^{Q62} / L_2 / \ k_5^{Q63} / L^7 / \ k_5^{Q64} / L_2 / \ k_6^{Q65} / L_2 / \ k_5^{Q66} / L_6$$

where L_6 is the length of the drifts before the LRD-Q61 and after LRD-Q66 quadrupoles, L_2 – the mutual distance of the quadrupoles of each triplets, L_7 – the distance between LRD-Q63 and LRD-Q64 quadrupoles, and k – the strength of the quadrupoles given by eq. (1). From the arrangement of this sub-section it can be seen that the strength of LRD-Q61, LRD-Q63, LRD Q64, and LRD-Q66 quadrupoles are the same. Also the strength of the LRD-Q62 and LRD-Q65 are the same. The total length of the third sub-section $L_{T,3}$ is 6.880 m. The fitting procedure to get the potentials at pole tips of quadrupoles is same as the fitting procedure in the case of the second sub-section. The transfer matrix T_3 at the end of this sub-section is

$$T_3 = \begin{bmatrix} 0.9648 & 0.5842 & 0 & 0 \\ 0.1182 & 0.9648 & 0 & 0 \\ 0 & 0 & 0.9648 & 0.5842 \\ 0 & 0 & 0.1182 & 0.9648 \end{bmatrix} \tag{6}$$

By comparing the matrices at the end of each sub-section this relation can be noticed

$$T_3 = -T_2 = T_1 \tag{7}$$

The distances L_6 and L_7 and the potentials at the pole tips of quadrupoles are: L_6 = 1.320 m, L_7 = = 2.640 m, $V_{Q61} = V_{Q63} = V_{Q64} = V_{Q66} = -0.9750$ kV, $V_{Q62} = V_{Q65} = 1.8183$ kV. The length ℓ and the half of the aperture R_0 of each quadrupole are same as in the previous sub-sections; *i. e.*, 20 cm and 5 cm, respectively. The total length of the third sub-section $L_{T,3}$ is 6.880 m. The beam optics of the third sub-section are shown in figs. 4(a and b).

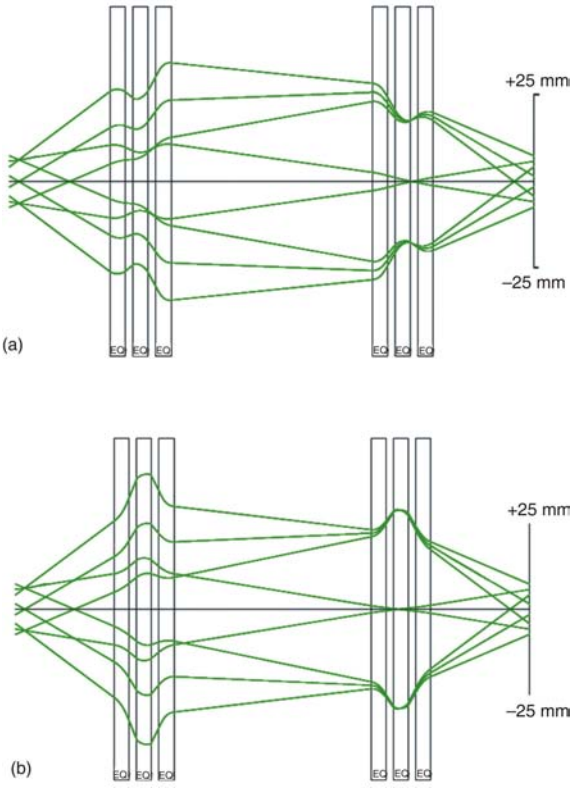

Figure 4. The beam optics of the third sub-section in the bending plane (a) and the beam optics of the third sub-section in the vertical plane (b)

The next sub-section of the beam line is dispersive section which consists of two spherical electrostatic deflectors; LRD-DE62 and LRD-DE71 (fig. 1) and quadrupole triplets (LR1-Q71, LR1-Q72, LR1-Q73) placed between them. The deflectors bend the beam for 90 degrees left and right (or up and down in the laboratory system). The bending radius of the deflectors ρ_0 is 40 cm.

The mid-plane radial field through the electrostatic deflector is given by [9, 11]

$$E(x) \quad E_0 \; 1 \quad n_1 \frac{x}{\rho_0} \quad n_2 \frac{x^2}{\rho_0^2} \quad n_3 \frac{x^3}{\rho_0^3} \quad n_4 \frac{x^4}{\rho_0^4} \quad n_5 \frac{x^5}{\rho_0^5} \tag{8}$$

where $\rho_0 = 0.400$ m is the bending radius (radius of trajectory of reference particle), E_0 – the strength of a constant electric field for which the reference particle can move along a circular optic axis of radius ρ_0 and n_i, $i = 1, 2, 3,\ldots, 5$ are the field indices. For the electric spherical deflector the field indices are: $n_1 = 2$, $n_2 = -3$, $n_3 = 4$, $n_4 = -5$, $n_5 = 6$ [9, 11].

The entrance of the first electrostatic deflector in this sub-section (LRD-DE62) is placed 40 cm away from the end of the previous sub-section and the exit of the LRD-DE71 deflector is 40 cm away from the start of the next sub-section. The quadrupole triplet between two deflectors (LRD-DE62 and LRD-DE71) is arranged as

$$0.64707\,\text{m} / \quad k_7^{Q71} / 0.27793\,\text{m} / \quad k_8^{Q72} \\ /0.27793\,\text{m} / \quad k_7^{Q73} / 0.64707\,\text{m}$$

where k is the strength of the quadrupoles given by eq. (1).

From the arrangement of this triplet it can be seen that the strength of LR1-Q71 and LR1-Q73 quadrupoles are the same. This forth sub-section is symmetric. The distances between quadrupoles and the potentials at the pole tips of quadrupoles in the triplet are results of the fitting procedure in which the energy dispersion D_E is minimized at the center of this sub-section, *i. e.*, at the center of the LR1-Q72 quadrupole. The potentials at the pole tips of quadrupoles are: $V_{Q71} = V_{Q73} = -2.4826$ kV, $V_{Q72} = 2.5241$ kV.

The transfer matrix $T_4^{0,C}$ at the center of this sub-section (center of LR1-Q72 quadrupole) in the case when the other sub-sections are excluded is

$$T_4^{0,C} = \begin{bmatrix} 0.4505 & 2.1068 & 0 & 0 & 1.0000 \\ 0.3604 & 0.5343 & 0 & 0 & 0.8000 \\ 0 & 0 & 5.8014 & 0.1649 & 0 \\ 0 & 0 & 1.3061 & 0.1352 & 0 \\ 0 & 0 & 0 & 0 & 1.0000 \\ 0 & 2.2197 & 0 & 0 & 0.3350 \\ 0 & 0.586\ 10^{6} & 0 & 0 & 0.5633 \\ 1.1943\ 10^{15} & 2.2197 & 0 & 0 & 0.2283 \end{bmatrix} \tag{9}$$

The deflectors are electrostatic and the energy and charge dispersions (the 6th and 8th numbers in the first column of the $T_4^{0,C}$ matrix) are equivalent, $D_E = -D_Z = 0.0$ m and the corresponding angular dispersions are $D_E = -D_Z = -2.22$ rad. The mass dispersions (lateral-the 7th number in the first column, and angular – the 7th number in the second column) are almost zero, $D_m = 0.0$ and $D_m \sim 10^{6}$

The transfer matrix T_4^0 at the end of this sub-section in the case when the other sub-sections are excluded is

$$T_4^0 = \begin{bmatrix} 0.5186 & 1.8982 & 0 & 0 & 0.1332\ 10^{14} \\ 0.3851 & 0.5186 & 0 & 0 & 0.7771\ 10^{15} \\ 0 & 0 & 0.5692 & 1.9133 & 0 \\ 0 & 0 & 0.3533 & 0.5692 & 0 \\ 0 & 0 & 0 & 0 & 1.0000 \\ 0 & 0.111\ 10^{14} & 0 & 0 & 0.6700 \\ 0 & 0 & 0 & 0 & 1.1266 \\ 0.6661\ 10^{15} & 0.222\ 10^{15} & 0 & 0 & 0.4566 \end{bmatrix} \tag{10}$$

The transfer matrix T_4 at the end of this sub-section in the case when the other sub-sections are included is

$$T_4 = \begin{bmatrix} 0.2753 & 2.1344 & 0 & 0 & 0.4441\ 10^{14} \\ 0.4329 & 0.2759 & 0 & 0 & 0.2221\ 10^{15} \\ 0 & 0 & 0.7556 & 1.5135 & 0 \\ 0 & 0 & 0.2736 & 0.7754 & 0 \\ 0 & 0 & 0 & 0 & 1.0000 \\ 0 & 0.111\ 10^{14} & 0 & 0 & 5.0004 \\ 0 & 0 & 0 & 0 & 5.4571 \\ 0.6661\ 10^{15} & 0.222\ 10^{15} & 0 & 0 & 0.4566 \end{bmatrix} \tag{11}$$

The beam widths in horizontal (bending) and transversal planes at the exit of this sub-section are

$$x \quad T_{11}x_0 \quad T_{21}a_0 \quad T_{31}y_0 \quad T_{41}b_0 \\ T_{61}\frac{\mathrm{d}E}{E} \quad T_{71}\frac{\mathrm{d}m}{m} \quad 4\,\text{mm} \tag{12}$$

$$y \quad T_{13}x_0 \quad T_{23}a_0 \quad T_{33}y_0 \quad T_{43}b_0 \\ T_{63}\frac{\mathrm{d}E}{E} \quad T_{73}\frac{\mathrm{d}m}{m} \quad 8\,\text{mm} \tag{13}$$

and the corresponding angles of these trajectories and optic axis in horizontal and vertical planes are

$$x \quad T_{12}x_0 \quad T_{22}a_0 \quad T_{32}y_0 \quad T_{42}b_0 \\ T_{62}\frac{\mathrm{d}E}{E} \quad T_{72}\frac{\mathrm{d}m}{m} \quad 16\,\text{mrad} \tag{14}$$

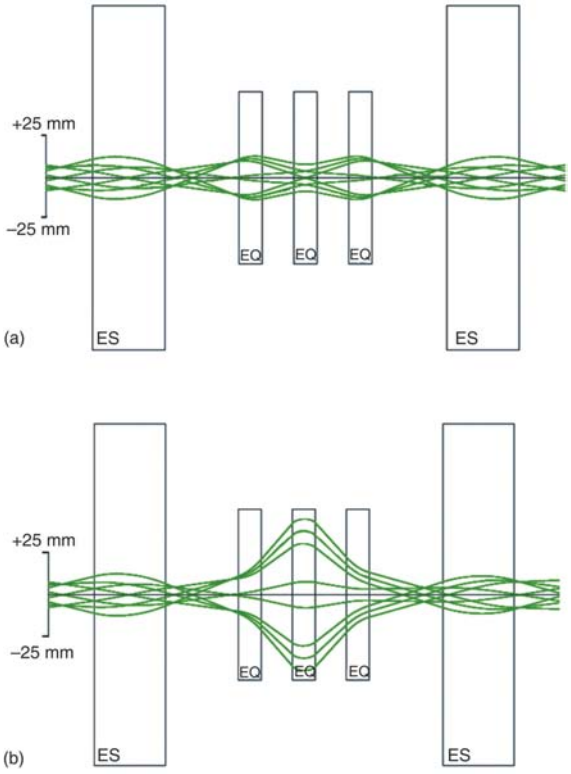

Figure 5. The beam optics of the forth sub-section in the bending plane (a) and the beam optics of the forth sub-section in the vertical plane (b)

$$y \quad T_{14}x_0 \quad T_{24}a_0 \quad T_{34}y_0 \quad T_{44}b_0 \quad T_{64}\frac{dE}{E} \quad T_{74}\frac{dm}{m} \quad 1\,\text{mrad} \tag{15}$$

The length ℓ and the half of the aperture R_0 of each quadrupole are same as in the previous sub-sections, *i. e.*, 20 cm and 5 cm, respectively. The total length of the fourth sub-section $L_{T,4}$ is 4.5066 m where the drifts of length 0.400 m before LRD-DE62 and after LRD-DE71 are also included.

The beam optics of the forth sub-section are shown in figs. 5(a and b).

Finally, the last sub-section consists of four electrostatic quadrupoles (ARD-Q11, ARD-Q12, ARD-Q13, and ARD-Q14; (fig. 1) arranged in a symmetrical way (like the first sub-sector), *i. e.*

$$L_8 / \quad k_{11}^{Q11} / L_2 / \quad k_{12}^{Q12} / L_9 / \quad k_{12}^{Q13} / L_2 / \quad k_{11}^{Q14} / L_8$$

where L_8 is the length of the drift before ARD-Q11 and after ARD-Q14 quadrupoles, L_2 – the distance between ARD-Q11 and ARD-Q12 quadrupoles (distance between ARD-Q13 and ARD-Q14 is also L_2), L_9 – the distance between ARD-Q12 and ARD-Q13 quadrupoles, k – the strength of the quadrupole given by eq. (1). From the arrangement of this sub-section it can be seen that the strength of ARD-Q11 and ARD-Q14 quadrupoles are the same but with opposite sign. Also the strength of ARD-Q12 and ARD-Q13 quadrupoles are the same but with opposite sign. The potentials at pole tips of all quadrupoles are fitted to get the beam size in both transversal planes equal as it is at the beginning of the beam line, *i. e.*, $x = x_0 = 6$ mm and $y = y_0 = 6$ mm and, also, the matrix elements σ_{21} and σ_{43} of the beam matrix have to be zeroed; to ensure the beam waist at the end of this section. The matrix T_5 at the end of this sub-section, *i. e.*, at the end of the beam line is

$$T_5 = \begin{bmatrix} 0.0218 & 2.2198 & 0 & 0 & 0.4441\ 10^{14} \\ 0.4503 & 0.0217 & 0 & 0 & 0.222\ 10^{15} \\ 0 & 0 & 0.9236 & 0.9478 & 0 \\ 0 & 0 & 0.1578 & 0 & 0 \\ 0 & 0 & 0 & 0 & 1 \\ 0.2489\ 10^{15} & 0.116\ 10^{14} & 0 & 0 & 6.0005 \\ 0 & 0 & 0 & 0 & 6.4572 \\ 0.2777\ 10^{15} & 0.2777\ 10^{15} & 0 & 0 & 0.4566 \end{bmatrix} \tag{16}$$

The distances L_8, L_9, and the potentials at the pole tip of quadrupoles are: $L_8 = 1.000$ m, $L_9 = 1.000$ m, $V_{Q11} = -V_{Q14} = -1.3464$ kV, $V_{Q12} = -V_{Q13} = 1.6124$ kV. The length ℓ and the half of the aperture R_0 of each quadrupole are same as in the previous sub-sections, 20 cm and 5 cm, respectively. The total length of the fifth sub-section $L_{T,5}$ is 4.000 m.

Since the dispersion section consists of pure electrostatic deflectors, the energy and charge dispersions are equivalent (the 6th and the 8th numbers in the first column of T_5 matrix), $D_E = -D_Z = 0.0$ m. The same conclusion is for the angular energy and charge dispersions (the 6th and 8th numbers in the second column of T_5), *i. e.*, $D_E \quad D_Z \quad 0.0$ rad. The mass dispersion, lateral and angular (the 7th number in the first and second column, respectively, of the T_5 matrix) is zero, $D_m = 0.0$, $D_m \quad 0.0$.

The beam widths in horizontal (bending) and transversal planes at the exit of this sub-section are

$$x \quad T_{11}x_0 \quad T_{21}a_0 \quad T_{31}y_0 \quad T_{41}b_0 \quad T_{61}\frac{dE}{E} \quad T_{71}\frac{dm}{m} \quad 6\,\text{mm} \tag{17}$$

$$y \quad T_{13}x_0 \quad T_{23}a_0 \quad T_{33}y_0 \quad T_{43}b_0 \quad T_{63}\frac{dE}{E} \quad T_{73}\frac{dm}{m} \quad 7\,\text{mm} \tag{18}$$

and the corresponding angles of these trajectories and optic axis in horizontal and vertical planes are

$$x \quad T_{12}x_0 \quad T_{22}a_0 \quad T_{32}y_0 \quad T_{42}b_0 \quad T_{62}\frac{dE}{E} \quad T_{72}\frac{dm}{m} \quad 13\,\text{mrad} \tag{19}$$

$$y \quad T_{14}x_0 \quad T_{24}a_0 \quad T_{34}y_0 \quad T_{44}b_0 \quad T_{64}\frac{dE}{E} \quad T_{74}\frac{dm}{m} \quad 7\,\text{mrad} \tag{20}$$

The total length of the whole transport beam line is 25.8286 m and the beam optics is shown in fig. 6(a and b).

The potentials at the pole tips for each quadrupole are presented in tab. 1.

CONCLUSIONS

In this paper the detailed structure of the transport beam line design is proposed, quadrupoles and deflectors specifications in order to transport the beam from the optic adaptation point in the SPIRAL2 production building up to the adaptation point in the DESIR hall. The total length of the whole transport beam line is 25.8286 m. To reach the high efficiency of transport of the beam line it is designed in such way that the beam sizes, in both planes, at the end (adaptation point in the DESIR hall) are kept the same as they are at the starting point, *i. e.*, 6 mm.

ACKNOWLEDGMENT

This work was supported by the Ministry of Education, Science and Technological Development of the Republic of Serbia under Grants No. OI-171018.

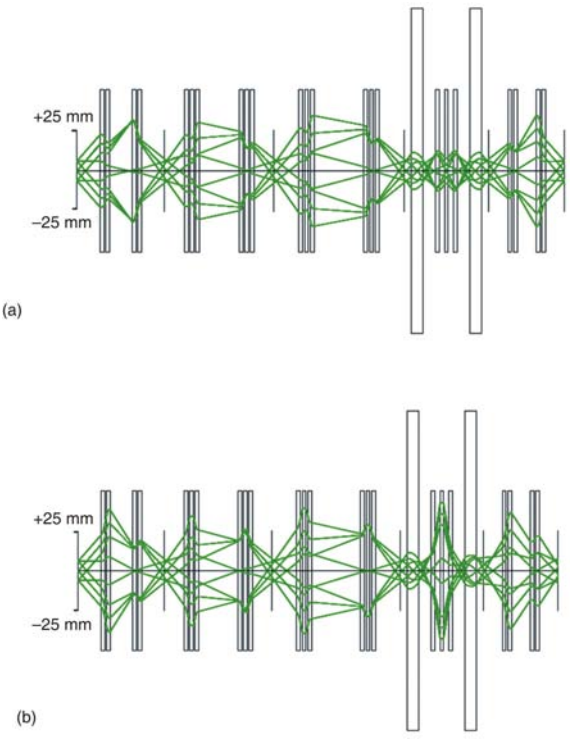

Figure 6. The beam optics of the proposed DESIR beam line in the bending plane (a) and the beam optics of the proposed DESIR beam line in the vertical plane (b)

Table 1. The potentials at the pole tips for the quadrupoles. In the laboratory frame the potentials should be taken with opposite sign

Quadrupole	*V* [kV]
LRD-Q501	1.24366
LRD-Q502	–1.46353
LRD-Q503	1.46353
LRD-Q504	–1.24366
LRD-Q505	1.0724
LRD-Q506	–1.9787
LRD-Q507	1.0724
LRD-Q508	1.0724
LRD-Q509	–1.9787
LRD-Q510	1.0724
LRD-Q61	0.9751
LRD-Q62	–1.8183
LRD-Q63	0.9751
LRD-Q64	0.9751
LRD-Q65	–1.8183
LRD-Q66	0.9751
LR1-Q71	2.48261
LR1-Q72	–2.52413
LR1-Q73	2.48261
ARD-Q11	1.34638
ARD-Q12	–1.61237
ARD-Q13	1.61237
ARD-Q14	–1.34638

REFERENCES

[1] Blumenfeld, Y., Radioactive Ion Beam Facilities in Europe, *Nucl. Instr. and Meth., B266* (2008), 19-20, pp. 4074-4079
[2] Tanihata, I., Radioactive Beam Science, Past, Present and Future, *Nucl. Instr. and Meth., B266* (2008), 19-20, pp. 4067-4073
[3] Henning, W., FAIr – An International Accelerator Facility for Research with Ions and Antiprotons, *Proceedings*, EPAC 2004, Lucerne, Switzerland, pp. 50-53
[4] Cornell, J., A Feasibility Study for a European Isotope-Separator-On-Line Radioactive Ion Beam Facility, Report to the European Commission, European Commission Contract No. HPRI-CT-1999-500001, Published by GANIL, December 2003, pp. 1-84, http://pro.ganil-spiral2.eu/eurisol/feasibility-study-reports/feasibility-study-final-report.pdf
[5] Voulot, D., *et al*., The REX-ISOLDE Collaboration, Radioactive Beams at REX-ISOLDE: Present Status and Latest Developments, *Nucl. Instr. and Meth., B266* (2008), 19-20, pp. 4103-4107, http://isolde.web.cern.ch/ISOLDE/REX-ISOLDE/index.html
[6] Andrighetto, A., *et al*., The SPES Multi-Foil Direct Target, *Nucl. Instr. and Meth., B266* (2008), 19-20, pp. 4257-4260
[7] Blank, B., *et al*., DESIR: the SPIRAL2 Low-Energy Beam Facility, Technical Proposal for SPIRAL2 Instrumentation, December 19, 2008, pp. 1-102 http://www.cenbg.in2p3.fr/desir/IMG/pdf/DESIR-Technical-Proposal-V090105.pdf
[8] Moscatello, M-H., Post Accelerator and Mass Separator for Eurisol, Report to the European Commission, European Commission Contract No. HPRI-CT-

1999-500001, Published by GANIL, December 2003, pp. D-45-D-67, http://pro.ganil-spiral2.eu/eurisol/feasibility-study-reports/feasibility-study-appendix-d
[9] Berz, M., Computational Aspects of Optics Design and Simulation: Cosy Infinity, *Nucl. Instr. and Meth., A298* (1990), 1-3, pp. 473-479, http://bt.pa.msu.edu/index_cosy.htm
[10] Toprek, D., Kurtikian-Nieto, T., DESIR High Resolution Separator at GANIL, France, *Nucl Technol Radiat, 27* (2012), 4, pp. 346-350
[11] Wollnik, H., Optics of Charged Particles, Academic Press, Fla., USA, 1987

Received on September 4, 2013
Accepted on September 9, 2014

Драган ТОПРЕК

ПРЕДЛОГ ТРАНСПОРТНЕ ЛИНИЈЕ СНОПА ЗА DESIR ПОСТРОЈЕЊЕ

У овом раду предложен је детељан дизајн транспортне линије снопа као и спецификација њених оптичких елемената: квадрупола и дефлектора, у циљу транспорта снопа од места где се јони производе, SPIRAL2 зграде, па све до уласка у DESIR халу. Сви оптички елементи су електростатички, тако да је њихово подешавање независно од масе јона. Прорачун је урађен помоћу COSY INFINITY програма у првом реду апроксимације и нису узети у обзир ефекти крајева оптичких елемената. Емитанце снопа на почетку транспортне линије (место производње јона у SPIRAL2 згради), у хоризонталној и вертикалној равни су 80 mm mrad. Транспортна линија је дизајнирана на начин да је величина снопа, како у хоризонталној, тако и у вертикалној равни, на њеном крају једнака величини снопа на њеном почетку, тј. хоризонтално и вертикално одступање трајекторије јона од оптичке осе на почетку и на крају транспортне линије једнако је и износи 6 mm. На овај начин постиже се већа ефикасност транспортовања снопа.

Кључне речи: линија снопа, емитанца, јонска оптика, COSY INFINITY